Radio Science, Volume 17, Number 4, pages 817–826, July–August 1982

Spectral parameter estimation of CAT radar echoes in the presence of fading clutter

Toru Sato[1] *and R. F. Woodman*[2]

Arecibo Observatory, Arecibo, Puerto Rico 00612

(Received September 15, 1981; revised March 15, 1982; accepted March 15, 1982.)

The 430 MHz, 2 MW radar at the Arecibo Observatory is currently being used as a stratospheric-troposheric (ST) radar. One of the problems in the automatic analysis of the signals come from the very large amplitude of the ground clutter echoes. The problem is agravated by the fading of these signals, which makes it difficult to discriminate them from the desired stratospheric returns. A parameter estimation technique that parameterizes the first three-spectral moments corresponding to the desired stratospheric signals as well as a few Taylor series coefficients of the auto-correlation function of the clutter is presented. The three first moments can be obtained in this manner even in the presence of clutter 50 dB stronger. The technique automatically takes care of instrumental and processing biases. Spectrum aliasing presents no problem. A sequence of fine altitude and high temporal resolution wind profiles is presented, showing the potential of the instrumental and technique for the study of stratospheric dynamics.

1. INTRODUCTION

The potential of powerful incoherent scatter and other powerful radars for the study of upper troposphere and lower stratosphere turbulence and and dynamics is now clearly established (see *Balsley and Gage* [1980] for a review). The radars at the Arecibo Observatory are not an exception; their possibilites were established by *Aso et al.* [1977], *Farley et al.* [1979], R. M. Harper (personal communication 1977), and more recently by *Woodman* [1980*a*, *b*]. The radar technique is based on scattering from clear air turbulence (CAT) fluctuations in index of refraction. The technique developed by *Woodman* [1980*a*] for the 430 MHz system has been used to obtain nearly 200 hours of observations, which, at the rate of 256 power spectra of 32 frequencies each, every 2 min., amounts to quite a significant amount of information. Automatic processing of the data into physically significant parameters is necessary. This paper describes the solutions given to the problems encountered in developing an automatic processing program of these data.

The main improvements to the Arecibo radar introduced by *Woodman* [1980*a*] are an improved range resolution (150 m) and the use of complementary codes. All statistical processing is performed on line in terms of power spectra. The power spectra for each altitude are estimated by time-averaging the absolute value squared of the discrete fourier transform (DFT) of 32 time consecutive points using a FFT algorithm. The resultant set of spectra are written on tape of further off-line reduction and analysis.

If it were not for the special nature of ground clutter signals, which contaminate the desired signals, further processing would involve simply an evaluation of the three first moments of the spectra, which are directly related to the intensity of turbulence, mean radial velocity of the medium and turbulent velocity variance, respectively. For the latter, it should be pointed out that instrumental effects, important in other radar installations, like beam-width and wind-shear spectrum broadening, are negligible at Arecibo. But, unfortunately, ground clutter at Arecibo is very large, many orders of magnitude stronger than the desired signals scattered from CAT. The problem is aggravated by the fact that the spectral signature of the clutter has finite width, which combined with the finite time widow (truncation) of the FFT technique used, produces a spectral spill over the clutter throughout the entire frequency window. This makes the separation of desired signal and clutter difficult. The intrinsic width of the ground clutter spectra is caused by variations in the air refractivity along the ray path.

[1] Now at Kyoto University, Kyoto, Japan.
[2] Now at the Instituto Geofísico del Perú, Lima, Perú.

Paper number 2S0413.
0048-6604/82/0708-0413$08.00

In the following sections, the nature of this 'spill-over' is examined. Then, as a solution of this problem, a nonlinear parameter estimation technique is described. This method utilizes a theoretical curve fitting procedure by using parameters that specify the shape of the clutter along with the desired three parameters for the CAT echoes. The theoretical functions are distorted in the same fashion as the data, which are distorted by the system and data processing algorithm. Then they are compared with the data and the parameters are adjusted until a best fit (using a minimum rms criteria) is obtained.

Results obtained by this technique are presented, illustrating the performance of the technique as well as the potential of the 430 MHz radar at Arecibo for the study of the short-time and fine-altitude dynamics of the troposhere and stratosphere.

2. EFFECT OF DATA PROCESSING

In the real time data processing, each consecutive 32 sampled data points are Fourier-transformed by using an FFT algorithm, squared and then averaged over 100 times. This method of averaged periodogram is a widely used technique to estimate the power spectrum of a long time series because of its high speed and minimum computer memory requirements. It is seldom realized, however, that this averaged periodogram does not converge to the true power spectrum, but gives a systematically distorted power spectrum. In this section we briefly examine the nature of this distortion.

Let $f(t)$ be a random process characterized by its frequency spectrum $F(\omega)$, to which corresponds an auto-correlation function $\rho(\tau)$. We will determine the effect of data processing in $F(\omega)$ through the effects on its transform, $\rho(\tau)$, because this effect is clearer in the time domain than in the frequency domain.

Consider a sampled series

$$f_N(j) = f(j\Delta) \tag{1}$$

where Δ is the sampling interval and j is an integer index. We truncate this series to obtain N points, which corresponds to applying a rectangular weight to $f_N(j)$.

$$\bar{f}_N(j) = f_N(j) \cdot w_N(j) \text{ for all } j\text{'s} \tag{2}$$

where

$$w_N(j) = 1 \qquad (1 < j < N)$$
$$w_N(j) = 0 \qquad (j < 0, j > N)$$

Applying a Fourier transform and squaring the results corresponds to auto-correlating $\bar{f}_N(j)$ in time. Thus

$$\begin{aligned}
&\bar{\rho}_N(k) = \langle \bar{f}^*_N(j) \cdot \bar{f}_N(j+k) \rangle \\
&\rho_N(k) = \rho_N(k) \cdot \langle w_N(j) \cdot w_N(j+k) \rangle \qquad \text{for all } k\text{'s} \\
&\rho_N(k) = \rho_N(k) \cdot (N-k)/N \qquad (0 < k < N) \\
&\rho_N(k) = \rho_N(k) \cdot (N+k)/N \qquad (-N < k < 0) \\
&\rho_N(k) = 0 \qquad (k < -N, k > N)
\end{aligned} \tag{3}$$

where $\rho_N(k)$ is a sampled series of $\rho(\tau)$ at interval Δ, and $\bar{\rho}_N(k)$ is an auto-correlation function taking only the effect of truncation into account. This effect is equivalent to multiplying $\rho_N(k)$ by a triangular weight, i.e., the auto-correlation function of $w_N(j)$. Figures 1*a* and 1*b* show examples of untruncated and weighted Gaussian auto-correlation functions, respectively. Two cases are shown corresponding to long (left) and short (right) correlation times as compared to the length of data. They correspond to typical correlation times for fading clutter and signal from CAT, respectively. At Arecibo, the length of the data window was chosen on the basis of the signal correlation time. This caused a severe truncation of the ground clutter contribution, which has a much longer correlation time than the signal.

Besides the triangular weight effect, we automatically use a sampling rate of $1/\Delta$ in the frequency domain when using a FFT algorithm, which causes an additional problem. The sampling in frequency corresponds to convolving $\tilde{\rho}_N(k)$ with a series of delta functions of interval $N\Delta$, thus producing an overlapping periodicity in the auto-correlation function, since the entire length of the triangular weights $2N\Delta$ is twice as long as the interval. We get finally,

$$\tilde{\rho}_N(k) = \rho_N(k) \cdot (N-k)/N + \rho_N(k-N) \cdot k/N \qquad (0 \le k < N) \tag{4}$$

and periodic outside this range with period N.

Figure 1*c* shows the effect of this convolution which has the same effect as folding 1*b* at the $N/2$ point and adding the folded part to the first half.

Figure 2 shows these effect in the frequency domain for the case of long correlation time shown in Figure 1. The solid line and dots correspond to Figures 1*a* and 1*c*, respectively. We can easily see that, even when the true power spectrum has a very narrow shape, the FFT algorithm described above has the effect of spilling high-frequency components

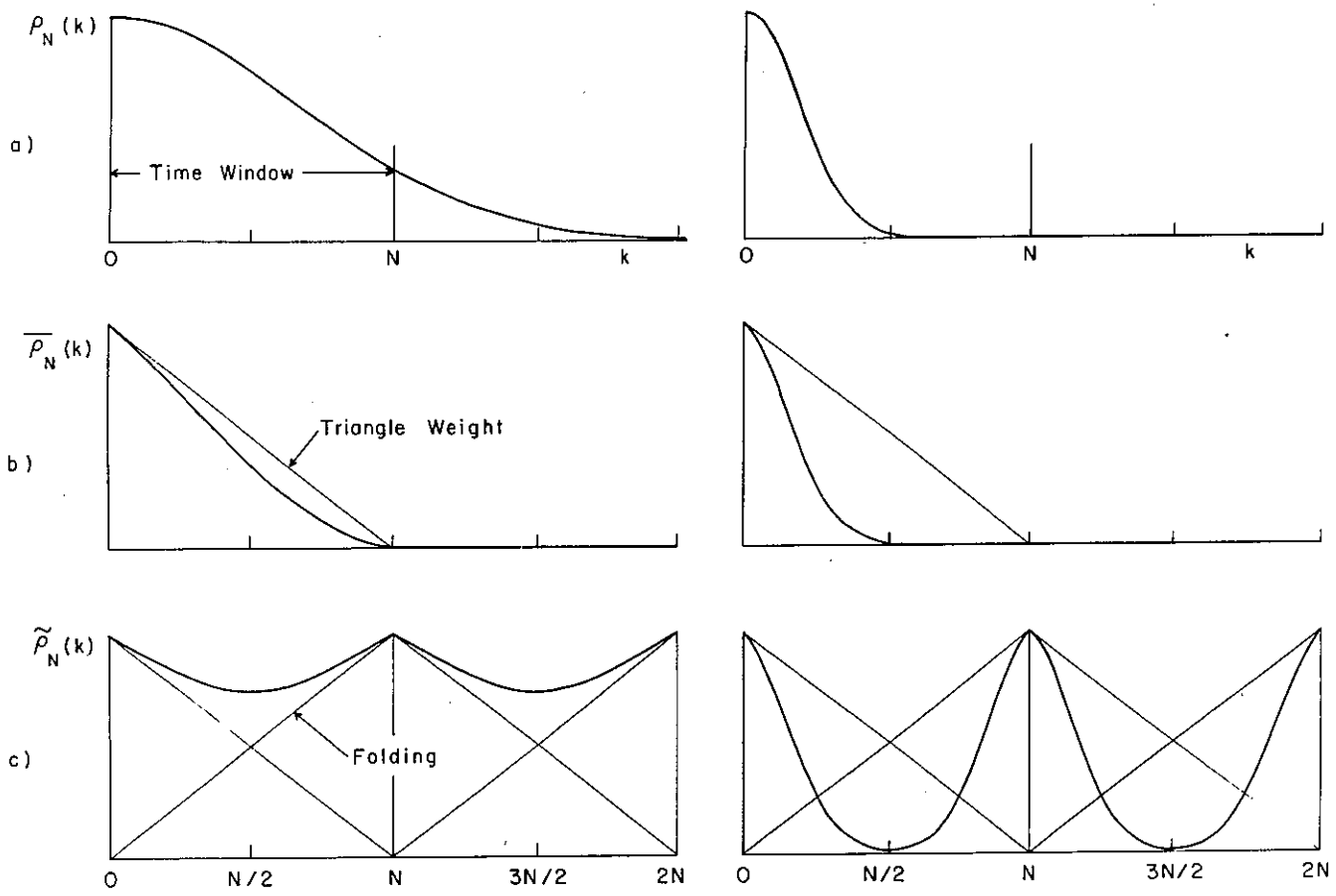

Fig. 1. Effect of processing distortion on the auto-correlation function caused by the periodogram operation using a FFT algorithm for two cases, where the correlation time is longer (left) and shorter (right) than the length of data. (*a*) Represents the actual correlation function of the signal. (*b*) The effects of truncation. (*c*) The effect of sampling in the frequency domain.

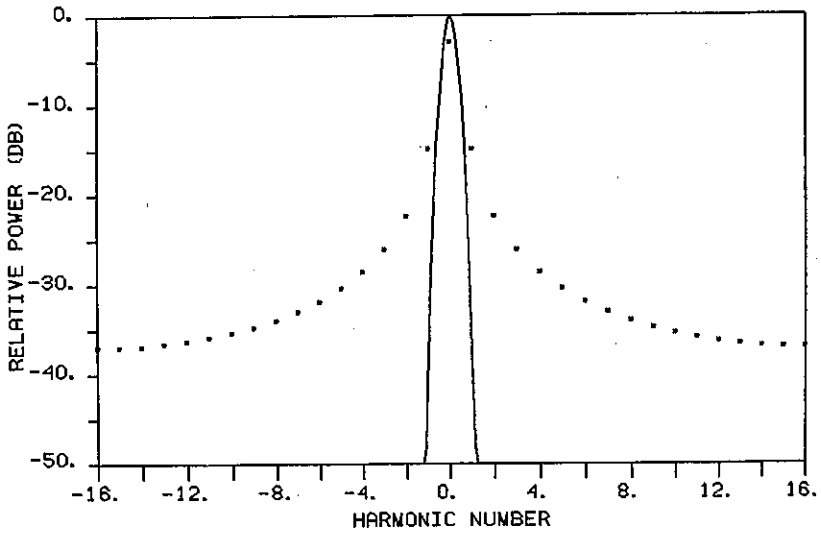

Fig. 2. Effect of the processing distortion on the power spectrum. The solid line shows the original spectrum and the dotted line shows the distorted spectrum.

over the entire frequency range. The high-frequency components come from the discontinuities at the apex as well as the base of the triangular weighting function.

Although this small amount of spill over is not a serious problem for most cases, this has a large effect for our case where the ground clutter is 10–50 dB stronger than the desired CAT echoes.

It is interesting to note that in the case of non-fading clutter, i.e., when the auto-correlation function is a constant, the effect of truncation and folding cancel each other, and the resultant $\bar{\rho}_N(k)$ is equal to $\rho_N(k)$. Thus, non-fading ground clutter affects only the center zero frequency with no spill over effect.

3. NONLINEAR PARAMETER ESTIMATION TECHNIQUE

As we have seen in the previous section, the existence of a very strong fading clutter under the effect of systematic distortion due to data processing makes it difficult to estimate the desired spectral parameters from the data. Therefore, it becomes quite important to estimate the spectral parameters of not only the signal echo, but also the fading clutter components. Here we describe the application of a nonlinear curve fitting technique to this problem.

The outline is as follows. First, we assume the theoretical function shape of the power spectral components of ground clutter and the desired CAT echo. Second, we distort it in the same fashion as described in the previous section. Then we compare this theoretically generated power spectrum with the observed one in least-squares manner to determine the optimum set of parameters. In reality, fitting is done in the time domain since the distortion is easier to apply in the time domain than in frequency domain. Distortion involves only a multiplication and folding in the former, but a lengthy convolution in the latter.

By applying the processing distortion to the theoretical autocorrelation function, we can take this effect into account, so that the estimated parameters are free from processing biases. Another advantage of the theoretical curve fitting is that we can obtain a better frequency resolution than the sampling interval in frequency. In fact we can obtain spectral width estimates as narrow as necessary, including single frequency spectral components like the non-fading component of clutter. This is an advantage that is normally associated with the maximum entropy method (MEM). Our approach is in fact better than the MEM, since we use previous knowledge about the nature of the signals, rather than assuming ignorance about the shape of the truncated tail of the auto-correlation function, which is the basis of MEM.

In our case, we can safely assume that the auto-correlation function of clutter can be approximated by the first few terms in a Taylor series expansion, since the correlation time is much longer than the maximum time lag. Also, since our main purpose is to get the first three spectral moments of the signal, we can assume a Gaussian shape with a linear phase for the signal contribution to the correlation function. This assumption is supported further by the central limit theorem, the independence of the scattering centers within the scattering volume, and the nature of the velocity distribution in a turbulent medium.

The curve fitting technique used to compare the theoretical and observed auto-correlation function is a general technique known as the non-linear least-squares fitting procedure [see, e.g., *Bard*, 1974]. The principle is to minimize the variance.

$$v(\mathbf{P}) = \sum_{k=1}^{N} \{\tilde{\rho}_N(k; \mathbf{P}) - R_N(k)\}^2$$

under certain conditions. Here R_N and $\tilde{\rho}_N$ are observed and distorted theoretical auto-correlation functions, respectively. $\mathbf{P}$ is the parameter vector that contains the following elements: the unfading clutter power, three even coefficients in the Taylor series expansion of the fading component of the clutter auto-correlation function, and the three parameters that define the Gaussian signal auto-correlation function (power, Doppler shift, and width). In addition, a slight Doppler shift for the fading component was found necessary to account for small statistical fluctuations in the estimate. Furthermore, a second Gaussian peak is introduced at certain altitudes to take care of secondary peaks produced by ocean clutter and sidelobe contamination from lower altitudes, as discussed later.

The necessary conditions for (5) to be minimized are

$$\sum_{k=1}^{N} \left\{\tilde{\rho}_N(k; \mathbf{P}) - R_N(k)\right\} \cdot \frac{\partial \tilde{\rho} N}{\partial P_j} = 0 \qquad j = 1, \ldots, M \qquad (6)$$

where M is the number of parameters. Equation (6) is nonlinear in terms of $\mathbf{P}$, therefore difficult (if not impossible) to solve directly. However, it can be approximately solved by expanding $\tilde{\rho}_N$ around some

initial value of $\mathbf{P}_0$ and taking up to the first order term.

$$\tilde{\rho}_N(k; \mathbf{P}_0 + \delta\mathbf{P}) \simeq \tilde{\rho}_N(k; \mathbf{P}_0) + \sum_{j=1}^{M} \delta P_j \frac{\partial \tilde{\rho}_N}{\partial P_j} \tag{7}$$

By substituting (7) into (6) we obtain

$$\mathbf{M} \cdot \delta\mathbf{P} = \mathbf{C}$$

where

$$M_{ij} = \sum_{k=1}^{N} \frac{\partial \tilde{\rho}_N}{\partial P_i} \cdot \frac{\partial \tilde{\rho}_N}{\partial P_j}$$

$$C_j = \sum_{k=1}^{N} \{R_N(k) - \tilde{\rho}_N(k; \mathbf{P}_0)\} \frac{\partial \tilde{\rho}_N}{\partial P_j}$$

Equation (8) can be solved for $\delta\mathbf{P}$

$$\delta\mathbf{P} = \mathbf{M}^{-1} \cdot C \tag{9}$$

This procedure is iterated by replacing $\mathbf{P}_0$ by $\mathbf{P}_0 + \delta P$ until $\mathbf{P}$ converges to some value, or $\delta\mathbf{P}$ becomes small enough.

Equation (6), however, has in general more than one solution, out of which only one is desirable. This ambiguity is solved by giving a proper initial guess and by setting constraints on parameters that prevent physically meaningless values like negative power or width. Additional constraints are set using the knowledge that the spectrum of clutter is always very narrow and almost symmetrical.

The initial set of $\mathbf{P}_0$ are obtained as follows. The unfading component of clutter is estimated from the dc value of the data, which is evaluated and recorded on real time. The fading clutter power and its width are estimated by assuming no signal power in the observed autocorrelation function. The function shape is set to be Gaussian, although it is later let free in shape for the fitting. The signal power, Doppler shift, and width of the desired signal are estimated from the asymmetric part of the observed power spectrum, taking advantage of the fact that the clutter component is almost symmetric. It has been found by experience that above procedures provide a fairly good guess.

4. RESULTS

Figure 3 shows some examples illustrating the quality of the fitting procedure. They are displayed in the frequency domain for convenience. The dots are the observed spectral points, the thick line is the fitted curve, and the thin line shows the desired signal contribution to the spectrum. The abscissa expresses

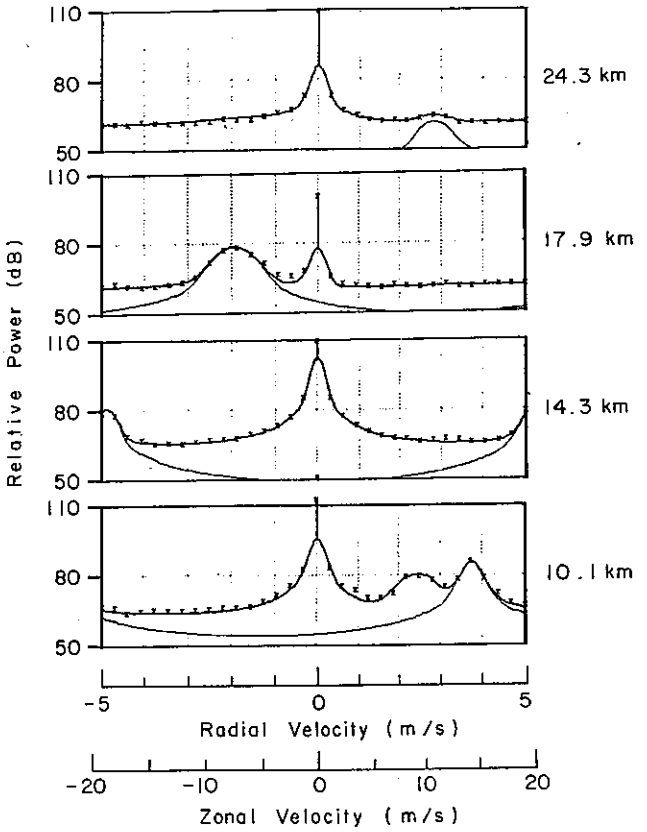

Fig. 3. Examples of theoretical curves fitted at four different altitudes. The dotted, the thick, and the thin line stand for the data, the fitted spectra, and the CAT contribution, respectively. The vertical line at zero Doppler shift shows the unfading clutter component.

both the radial velocity (15° off zenith) and zonal velocity.

The spectrum corresponding to 10.1 km illustrates an additional problem common at low altitudes. Here the power spectrum frequently shows a multi-humped shape, which is due to a 'sidelobe' of the pulse code corresponding to very strong echoes from lower altitudes. In principle, the complementary code scheme used has no sidelobes. However, nonlinearity and limited transmitter bandwidth cause some ringing at the tail of each pulse, which gives effective sidelobes of about −25 dB. Another Gaussian with a linear phase is added to the theoretical function to compensate this effect when fitting is not good without it. The spectra at 14.3 km and 17.9 km show two examples where the desired signal component is strong. The aliasing seen at 14.3 km due to a strong zonal wind causes no problem in fitting, since its effect is automatically taken care of in the time domain. The spectrum at 24.3 km shows an example

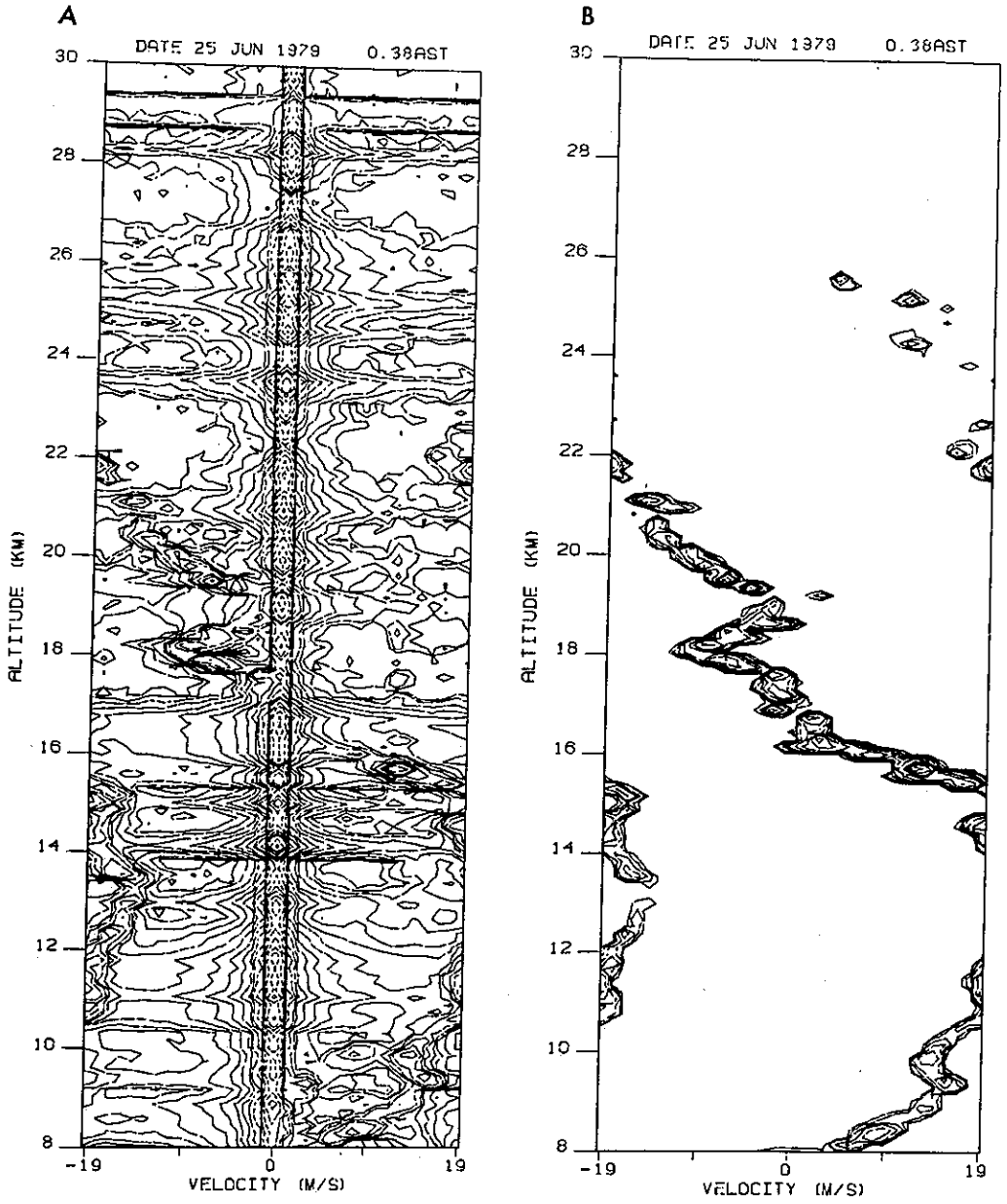

Fig. 4. Contours of equal spectral power density versus height and frequency (in the scale of zonal velocity). (*a*) The data before processing, (*b*) the CAT echo component extracted from the data. Contours are drawn every 3 dB. The spectra at 10–16 km and above 22 km are aliased because of strong zonal winds.

of a very weak signal, in which signal-to-clutter (S/C) ratio is about −50 dB. It is possible to get good fit even for a worse S/C ratio than in this case, provided that the Doppler shift of the signal echo is not too small.

At higher altitudes, a second and usually weak echo with a constant Doppler shift as a function of height is observed. It is probably an echo from ocean waves. The extra Gaussian function, which is used at low altitude to compensate for sidelobe echoes, is used at higher altitudes to compensate for this second component.

Figure 4 shows an example of the power spectra before and after processing. It is displayed in the form of contours of equal power density in a logarithmic scale and as a function of altitude and frequency. Contours are drawn every 3 dB starting slightly above the minimum detectable level. The contours for the spectra after processing are reproduced by using the echo power, Doppler shift and the

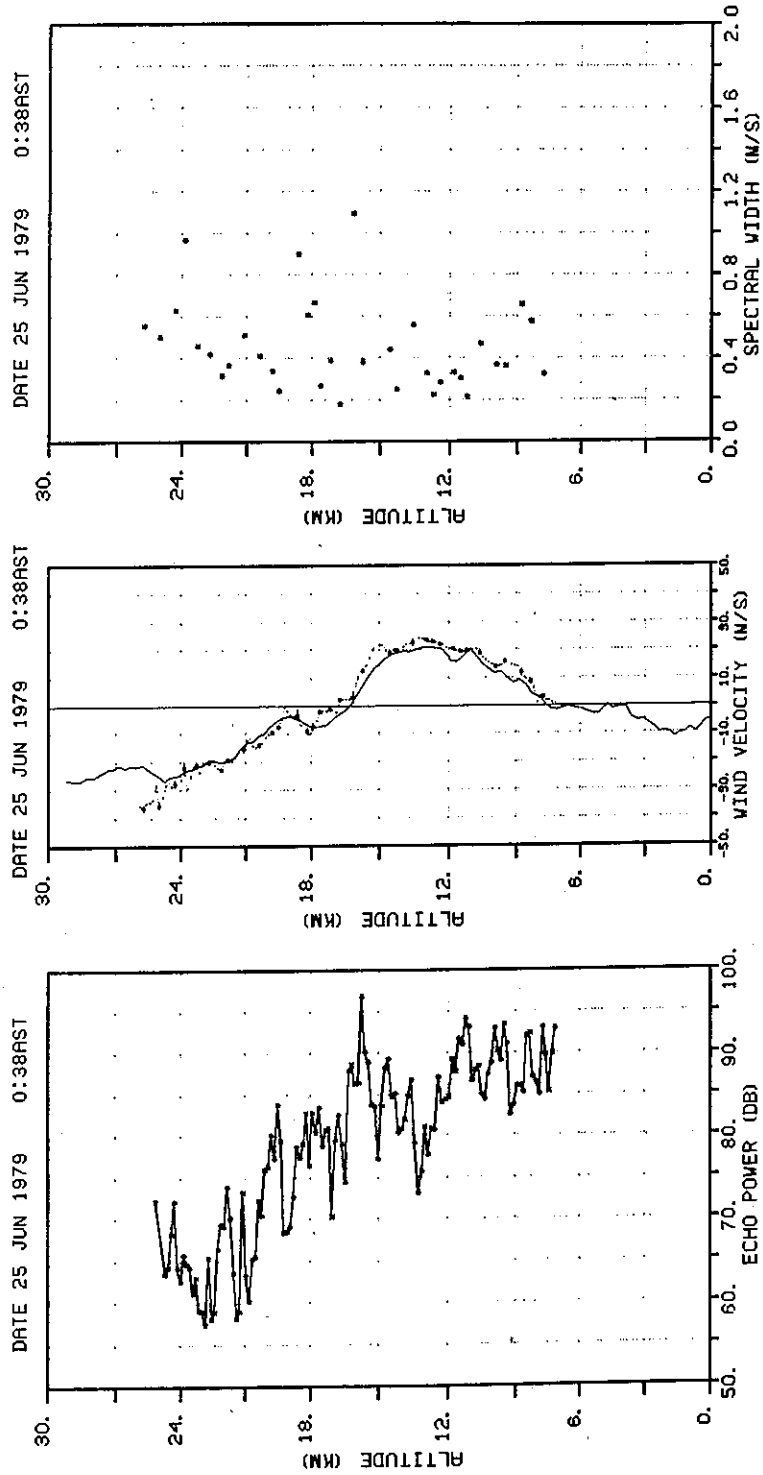

Fig. 5. Height profiles of CAT echo power, zonal wind velocity, and the spectral width obtained by nonlinear fitting. The velocity and width are plotted only for altitudes where the echo power is a local maxima. The continuous line in the velocity plot is the zonal wind profile observed by a meteorological balloon at 29 AST on June 24, 1979.

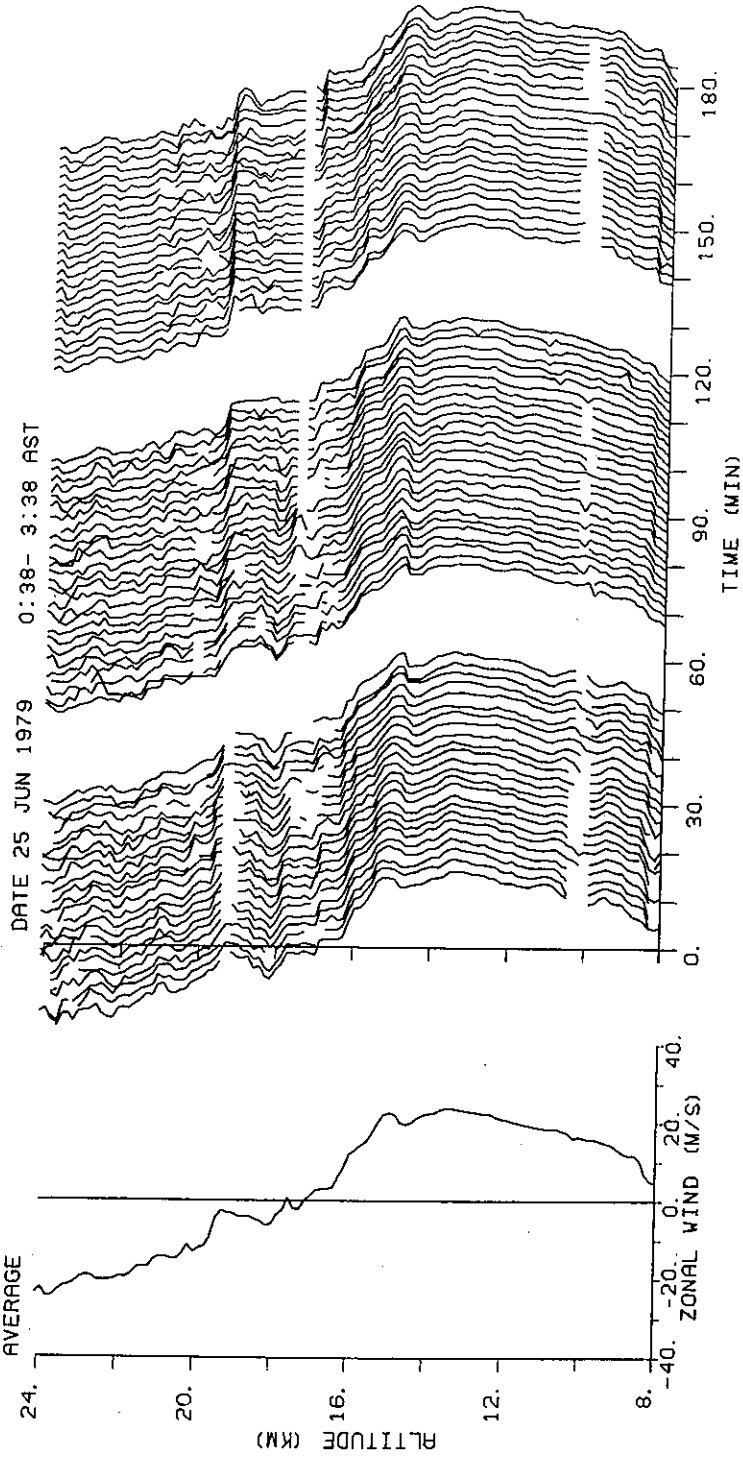

Fig. 6. Average and individual zonal wind profiles obtained every 2 min over a 3-hour period. The spacing between adjacent profiles corresponds to 3 m/s.

spectral width obtained by the fitting procedure described in the previous section. A uniform gradient of 2 dB/km is subtracted from the processed spectra to reduce the number of contours at low altitudes. The antenna beam was tilted 15° from zenith toward the East. The abscissa is scaled in zonal wind velocity assuming no vertical velocity.

It is evident from the figure that the technique works successfully in discriminating against the undesired spectral components, except for those cases where the CAT echo power is weak and the Doppler shift of the CAT echo is very small.

Figure 4*b* was reproduced here only to illustrate the performance of the fitting procedure. In practice, it is less laborious and more appropriate to obtain only the profiles of each parameter since the spectral profiles are already parameterized in the process of fitting. Figure 5 shows the height profiles of echo power, zonal wind velocity, and the spectral width (in units of radial velocity fluctuations) corresponding to the spectral profiles shown in Figure 4. Spectra at altitudes where echo power is much weaker than the neighboring heights are probably affected by finite bandwidth and residual sidelobes of the code, therefore the velocity and spectral width profiles are dotted only at the altitude of local power maxima.

Each power maxima can be interpreted as corresponding to the detection of a turbulent layer at the corresponding altitude. Profiles like the one shown in Figure 5*a* can and will be used for the statistical determination of turbulence occurrence, its dynamics and its relation to the background wind profiles.

Figure 5*a* indicates a highly discrete stratified structure showing the strongest layer at the tropopause height (as deducd from the meteorological balloon data). The vertical shear of the zonal wind is also the maximum at this altitude.

The thin continuous line in Figure 5*b* shows the zonal wind as measured by a meteorological balloon launched from the San Juan airport, 75 km away from the radar site, 4 hours before the radar measurement. The wind velocities measured by the radar and the balloon show a very good agreement in spite of the fairly large time and space difference.

Spectral widths are of the order of 0.2 to 0.6 m/s, in good agreement with previous measurements made at Jicamarca, Perú [*Woodman and Guillen*, 1974]. They are related to the turbulent velocity variance, thus to the turbulent kinetic energy in the layer. Although there is some contribution to the spectral width due to wind shear in regions where it is large, e.g., at 16 km. Beam width is also potentially capable of producing some broadening of the spectral width, but not with the narrow beam of the Arecibo antenna.

The greatest advantage of the radar measurement over other meteorological apparatus is that the radar offers high-resolution continuous data not only in altitude, but in time. In our case, height and time resolutions are 150 m and 2 min., respectively. Figure 6 shows the average and consecutive zonal wind profiles over a three-hour period. The scale for wind velocity is the same for the average and individual profiles. The spacing between two consecutive profiles corresponds to 3 m/s. Altitudes where the magnitude of the estimated wind velocity falls below 1 m/s, or where the fitting was not successful because of the effect of code sidelobe interference, are eliminated. Figure 6 indicates that the temporal variation of the wind profile was relatively slow and the wind system was very stable on this case. The consistence from one profile to the next also confirms the self-consistency of the wind velocity inferred by the radar. We can calculate an upper limit for the statistical fluctuations of the estimated velocity by assuming that all short period fluctuations are due to a statistical error. The standard deviation of the velocity, obtained by applying a high-pass filter to the time series of the wind velocity at each height, ranges from about 0.3 m/s at 8 km to about 1 m/s at 24 km for the zonal velocity, corresponding to 0.08 m/s to 0.26 m/s for the radial velocity.

This value is still larger than the theoretical estimate for this error [*Woodman and Guillen*, 1974], partly because it contains the short period geophysical fluctuations of wind velocity. Nevertheless, it gives a good indication of the reliability on the stratospheric radar measurements of wind velocities.

5. CONCLUSION

The analysis technique and a part of the results obtained from CAT radar echoes from higher troposphere and lower stratosphere have been presented. First, the effect of processing distortion caused by the periodogram method by using FFT algorithm on the slowly fading ground clutter echo was discussed. It is shown that a very narrow clutter spectrum can spill over the entire frequency range if the time window for every DFT is shorter than the fading clutter correlation time, affecting largely the estimation of the CAT spectrum contribution, especially when the

latter is a few tens of dB weaker than the former. Nevertheless, a good understanding of these process makes it possible to extract the desired signal contribution from the spectrum.

A nonlinear least squares fitting procedure was used to parameterize the observed power spectrum in terms of CAT echo power, Doppler shift, spectral width, and the parameters which specify the shape of the clutter component. The effect of clutter spill-over and other effects of processing were taken care of by distorting the theoretical function, in the same manner as done by the FFT algorithm, before comparing it with the data.

This technique has proved to work successfully for most cases. A good coincidence was found between the zonal wind velocity determined by the radar and the meteorological balloon. Time variation of the wind velocity profiles at 2-min interval shows a very smooth change giving an estimate of the statistical error in zonal wind to be less than 0.3–1.0 m/s depending on altitude.

This time resolution and accuracy will allow us to study wind dynamics from the shorter period, close the Brunt-Väisälä frequency, to the longest periods corresponding to tidal and planetary wave motions.

The height resolution of 150 m allows us to detect and characterize statistically the occurrence of turbulent layers, and resolve its separation as a function of altitude.

Acknowledgments. The Arecibo Observaroty is part of the National Astronomy and Ionosphere Center, which is operated by Cornell University under contract with the National Science Foundation. This work was supported partially by the National Aeronautics and Space Administration under NASA order no. W-14, 569.

REFERENCES

Aso, T., S. Kato, and R. M. Haroer (1977), Arecibo middle atmosphere experiment, *Geophys. Res. Lett.*, *4*, 10–12.

Balsley, B. B., and K. S. Gage (1980), The MST radar technique: Potential for middle atmospheric studies, *Pure Appl. Geophys.*, *118*, 452–493.

Bard, Y. (1974), Nonlinear parameter estimation, Academic, New York.

Farley, D. T., B. B. Balsley, W. E. Swarts, and C. La Hoz (1979), Winds aloft in the tropics measured by the Arecibo radar, *J. Appl. Meteorol.*, *18*, 227–230.

Woodman, R. F. (1980*a*), High altitude-resolution stratospheric measurements with Arecibo 430-MHz radar, *Radio Sci.*, *15*, 2, 417–422.

Woodman, R. F. (1980*b*), High altitude-resolution stratospheric measurements with the Arecibo 2380-MHz radar, *Radio Sci.*, 15, 2, 423–430.

Woodman, R. F., and A. Guillen (1974), Radar observations of winds and turbulence in the stratosphere and mesophere, *J. Atmos. Sci.*, *31*, 493–505.